REVIEW OF METHODS TO ESTIMATE FLUVIAL SUSPENDED SEDIMENT CHARACTERISTICS FROM ACOUSTIC SURROGATE METRICS

Mark N Landers, P.E., U.S. Geological Survey, Atlanta GA, landers@usgs.gov

INTRODUCTION

Sedimentation (erosion, transport, and deposition) is a primary and growing environmental, engineering, and agricultural issue around the world. Environmental impacts of sedimentation include loss of benthic aquatic habitat, changes in photosynthesis and visibility, and impacts from contaminants attached to and transported by sediments (Wood and Armitage, 1997). Sediment is the third most frequent cause of impairment in EPA's 303(d) list, accounting for 6,749 stream segments in the United States (U.S. EPA, 2008). Engineering challenges due to sedimentation include reduced waterway values for flood-control, recreation, and navigation, and increased water-treatment costs. More recent engineering challenges include dam decommissioning and removal, stream restoration, and contaminated sediment removal. Sedimentation of arable lands is a primary threat to agricultural productivity and sustainability.

Informed solutions to these problems require improved understanding of sedimentation; however the amount of fluvial sediment data collected in recent decades has decreased. The number of sediment monitoring stations operated by the U.S. Geological Survey (USGS) with consistent and comparable data has declined by about three-fourths from 1982 to 2008 (Gray and Gartner, 2009). This decline can be attributed to many factors including cost, manually intensive methods, and safety considerations. Suspended-sediment surrogates, including acoustic, turbidity, and laser diffraction metrics, have the potential to provide sediment data using methods that are more accurate, of higher spatial and temporal resolution, and with less manually intensive and dangerous procedures. If the surrogates can be developed from acoustic devices that are already being deployed in rivers, then costs may be lower than traditional methods.

Measurements of fluvial suspended-sediment characteristics using surrogates can be made with temporal resolutions of less than one minute (including averaging and filtering). High temporal resolution data are needed to describe processes in smaller and urbanizing watersheds where flow and sediment conditions change rapidly. Acoustic methods can measure (ensonify) and delineate a larger volume of water than traditional methods, and the profile of acoustic data can provide profiles of sediment concentration, resulting in much better spatial resolution. In addition to concentration, multi-frequency acoustics and laser diffraction may be used to measure changes in sediment-size characteristics. Sediment size can be indicative of absorbed, sediment-associated contaminants, biological impacts, and sediment sources (Horowitz, 1991, Wood and Armitage, 1997).

Much of the research into suspended-sediment surrogates has been conducted in marine environments rather than fluvial environments. In fluvial environments, turbidity (nephelometric and optical backscatter sensors) has been used as a sediment surrogate for several decades (Walling, 1977; Downing et al, 1981; Lewis, 1996; Uhrich and Bragg, 2003; Horowitz et al., 2008; Rasmussen et al, 2009); although its limitations have also been broadly documented (Conner and De Visser, 1992; Downing, 1996; Sutherland et al., 2000; Jean et al., 2008; Landers, 2003). Acoustic surrogates of suspended sediment concentration (SSC) have been broadly investigated using principles of acoustic scattering and attenuation by SSC, as discussed in greater detail in the following section (Crawford and Hay, 1993; Gartner, 2004; Thorne et al., 1991; Topping et al., 2007). Two general methods have been developed for using acoustic surrogates of sediment properties, and these have rarely been resolved mathematically. Also, there has been some confusion about the effects of coarser sediment fractions on acoustic attenuation. The relation of acoustic metrics to sediment characteristics is rendered complex and dynamic by the acoustic influence of other environmental and instrument properties.

This paper provides a thorough literature review of methods to estimate sediment characteristics from the acoustic metrics of attenuation and backscatter. The two principal methods of estimating sediment characteristics from acoustic surrogates are described and compared. Multi-cell and multi-frequency acoustic approaches also are reviewed. These methods are being evaluated in an ongoing project to determine fluvial suspended sediment characteristics by high-resolution, surrogate metrics of multi-frequency acoustic, turbidity, and laser-diffraction properties in the 260 square mile Yellow River watershed in metropolitan Atlanta, Georgia, USA.

ACOUSTIC SEDIMENT SURROGATES

Characterization of suspended sediment using backscatter and attenuation of acoustic signals in water has been described and developed for several decades (Urick, 1948, 1975, Flammer, 1962, Hay, 1983, Sheng and Hay, 1988, Flagg and Smith, 1989, Thorne et al., 1991, Hay and Sheng, 1992, Lynch et al., 1994, Thorne and Hardcastle, 1997, Holdaway et al., 1999, Gartner, 2004, Topping et al., 2006, Wall et al., 2006, Gray and Gartner, 2009). The basic principles are that acoustic waves passing through a water-sediment mixture will scatter and attenuate as a function of sediment, fluid, and instrument properties. The acoustic metrics of backscatter and attenuation relate functionally to sediment characteristics (concentration, size, and shape) within an ensonified volume after adjusting for the influence of fluid and instrument properties.

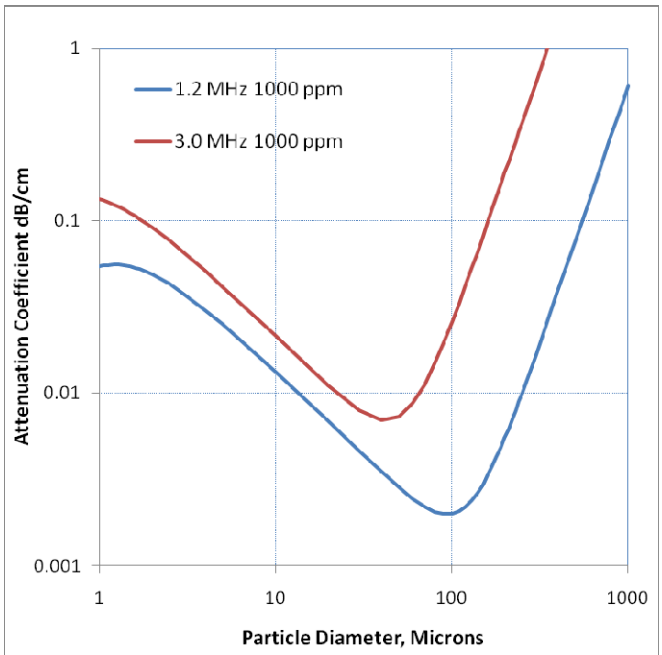

Figure 1. - Coefficient of acoustic attenuation due to suspended sediment and particle size, for 1.2 and 3.0 MHz frequencies at concentration of 1000 ppm from Urick's equation (1948)

Acoustic Attenuation Rayleigh (1896, § 334) developed the theory and expressions for the pressure disturbance (scattering) due to planer acoustic waves impinging on fluid spheres in an inviscid medium. Sewell (1910) derived expressions of energy loss (absorption) for rigid, fixed spheres in viscous fluid. Lamb (1916, § 296-298) extended Sewell's method for rigid spherical objects that are free to move in the sound field. Urick (1948) extended Lamb's theoretical absorption equation to include scattering and viscous loss components for a given concentration of spherical particles. Urick (1948) wrote his equation as a coefficient for the attenuation of acoustic energy by sediment, which is plotted in figure 1 and may be expressed in decibels per centimeter (dB/cm) as:

$$\alpha_S = SSC_V \left[k(\gamma - 1)^2 \left\{ \frac{s}{s^2 + (\gamma + \tau)^2} \right\} + \frac{1}{6}(k^4 a_s^3) \right] 4.34 \qquad (1)$$

where SSC_V is the dimensionless volumetric sediment concentration (SSC divided by sediment density), k is the wave number, $2\pi/\lambda$, λ is the wavelength in cm, γ is the specific gravity of the sediment, a_s is the mean sediment radius in cm, s is equal to $[9/(4\beta a_s)][1+1/(\beta a_s)]$, τ is equal to $[0.5+9/(4\beta a_s)]$, in which β is equal to $[\omega/2\upsilon]^{0.5}$, ω is $2\pi f$, f is frequency in hertz (Hz), υ is the kinematic viscosity of the water, in stokes, and 4.34 is the conversion from nepers to decibels for the attenuation. The first term of the sum within the brackets is the acoustic attenuation due to viscous losses and the second is the acoustic attenuation due to scattering losses. This form is dimensionally consistent and has been used by several subsequent researchers (Flammer, 1962; Hay, 1983; Gartner, 2004; Wall, et al., 2006).

Urick (1948) tested equation 1 with laboratory data using quartz and kaolinite particles with medium diameters of 2.2 and 0.9 microns (μm), respectively in frequencies of 1 to 15 megahertz (MHz) at a range of concentrations. Urick found good agreement between the equation and laboratory results and noted that viscous losses accounted for nearly all of the absorption for the small particle sizes investigated for 1 to 15 MHz frequencies.

Flammer (1962) tested Urick's theoretical expression for scattering attenuation, but did not investigate viscous losses because of equipment limitations for smaller particle sizes. Flammer conducted experiments over a range of frequencies from 2.5 to 25 MHz, and sediment size distributions with mean diameters from 44 to 1000 μm. Flammer developed an expression in additional to viscous and scattering losses for attenuation due to diffraction by particles where $\lambda << 2\pi a_s$. Flammer found 'reasonably good' agreement between measured and computed geometric mean sediment size for a range of sediment gradations.

Sheng and Hay (1988) investigated methods of estimating acoustic attenuation due only to scattering using data from four prior investigations, with most of the data coming from Flammer (1962). Their expression was further developed in Crawford and Hay (1993) and is shown in figure 2 and expressed as:

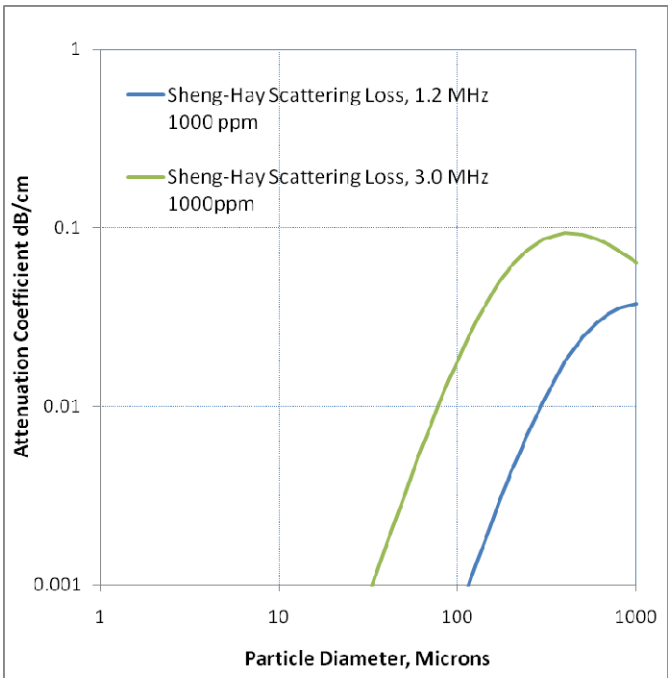

Figure 2. - Coefficient of acoustic attenuation due to suspended sediment and particle size, for 1.2 and 3.0 MHz frequencies at concentration of 1000 ppm from Sheng and Hay's equation (1988)

$$\alpha_s = SSC_v \left[\frac{k^4 a_s^3}{5(1 + 1.3k^2 a_s^2 + 0.24k^4 a_s^4)} \right] 4.34 \qquad (2)$$

where the terms are the same as in equation 1. This expression has been used by many authors investigating sediment surrogates in marine environments where particle sizes larger than 63 μm are dominant and thus viscous losses were regarded as negligible. (Thorne et al., 1991, Hay and Sheng, 1992, Thorne and Hardcastle, 1997, Holdaway et al., 1999, Thorne and Hanes, 2002).

In many fluvial environments the size distribution of suspended sediments may include significant fractions of both silt/clay (less than 63 μm) and sand (greater than 63 μm) sizes. Some investigators (*personal communication, Scott Wright, USGS*) including this author have replaced the scattering loss function in Urick's equation with that of Sheng and Hay to produce the following hybrid estimator of acoustic attenuation by SSC shown in figure 3 and equation 3.

$$\alpha_S = SSC_V \left[k(\gamma - 1)^2 \left\{ \frac{s}{s^2 + (\gamma + \tau)^2} \right\} + \left\{ \frac{k^4 a_s^3}{5(1 + 1.3k^2 a_s^2 + 0.24k^4 a_s^4)} \right\} \right] 4.34 \qquad (3)$$

where terms are defined the same as in equation 1. The viscous loss is due to shear at the fluid-particle boundaries because of a lag between the sound-wave induced vibration of the particle and that of the fluid. The magnitude of the viscous loss is a function of the particle surface area, sound frequency, fluid viscosity, and the ratio of particle to fluid density. From the left edge of the curves in figure 3, as the composite total surface area of suspended particles decreases with increasing particle size for a given suspended sediment concentration (SSC), there is a decreasing lag, shear, and viscous loss. Viscous losses are primarily due to the concentration of finer size particles while scattering losses are primarily due to coarser size particles. Minimum acoustic attenuation occurs at the transition

between viscous and scattering losses. The particle size associated with this minimum attenuation increases with decreasing frequency or increasing wavelength (figure 1). This minimum occurs, according to equation 1, at particle diameters of 91 and 41 μm for frequencies of 1.2 and 3.0 MHz, respectively, using 1,484 meters per second as the speed of sound in water.

Scattering loss is due to reradiation of the acoustic energy incident on a particle. Scattering loss is a function of the ratio of acoustic wavelength, λ, to particle circumference $2\pi a_s$. For $\lambda >> 2\pi a_s$ most of the scattered energy is reflected back toward the source, and scattering losses rise rapidly with increasing sediment size. As λ approaches $2\pi a_s$ scattering becomes complex and changes rapidly with sediment size and frequency (Urick, 1948; Flammer, 1962). Scattering attenuation reaches a maximum at particle diameters of about 1,050 and 425 μm for frequencies of 1.2 and 3.0 MHz, respectively. For $\lambda << 2\pi a_s$ half of the scattering propagates in the forward direction and the remainder scatters through all directions. Because of this physical relation between frequency and sediment size, there will be an optimal acoustic frequency for surrogate measures of sediment characteristics for a given particle size distribution.

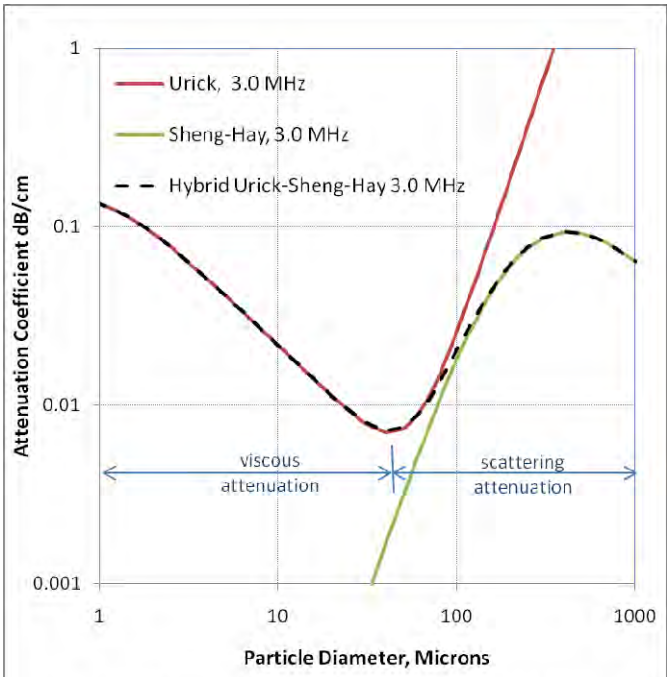

Figure 3 - Coefficient of acoustic attenuation due to suspended sediment and particle size, for 3.0 MHz frequencies at concentration of 1000 ppm from hybrid Urick-Sheng-Hay equation

Acoustic absorption varies linearly with SSC_V for a given frequency. Linear variation of absorption with concentration implies that the absorption effects from individual particles are independent, because the particles are 'far enough apart' so that the scattering from one does not affect that of its neighbors. This assumption has been proven valid for a range of sediment sizes for concentrations up to 10,000 milligrams per liter (mg/L) (Urick, 1948; Flammer, 1962; Sheng and Hay, 1988).

Recently some authors (Topping et al, 2007; Wright and Topping, 2010) have indicated that fine particles (less than 63 μm) have a more dominant affect than coarse particles on acoustic attenuation by sediments. As a general assumption, however, this does not appear to be supported by theoretical or experimental results. The relative contribution of silt-clay sediment (viscous losses) and sand sediment (scattering losses) to total attenuation will depend on the gradation of the sediment mixture in the sampled volume. For example, using equation 3, the total acoustic attenuation for a suspension of uniform 250 μm sand is equal to that for a suspension of uniform 9 μm silt, independent of concentration, for a 1.5 MHz system, and a speed of sound in water of 1,484 meters per second. Flammer's (1962) thorough and often cited work, which verified Urick's equation, used sediments sizes primarily in the fine sand range. Also, Thorne and Hanes (2002) note that for noncohesive sediments ensonified at MHz frequencies the scattering component dominates. This point is important, even though it may be academic in many applications where the effect of attenuation is negligible compared to acoustic backscatter.

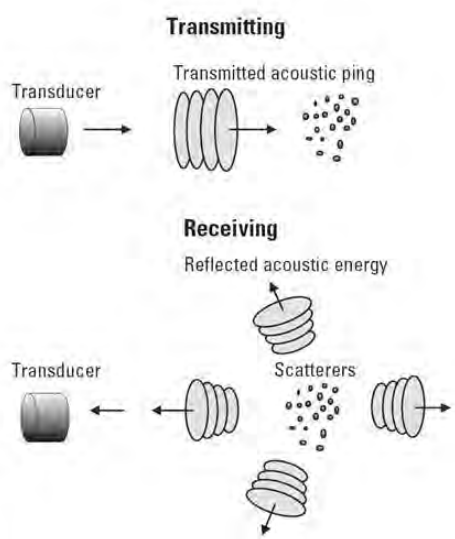

Figure 4 - Acoustic backscatter from suspended particles (from Simpson, 2001)

Acoustic Backscatter_Early investigations of acoustic surrogates relied on instruments with a separate sound source and receiver, rather than a

combined source and receiver such as modern transceivers (referred to here and typically as transducers). The transducer emits an acoustic pulse and then, after an interval just long enough to stop 'ringing', it receives the echoes backscattered from particles suspended in the acoustic path, as illustrated in the simplified diagram of figure 4. Acoustic doppler current profilers (ADCPs) measure the doppler shift in the frequency of the backscattered signal to determine the velocity of the scatters (assumed to equal water velocity) relative to the transducer. Two or three transducers at fixed beam angles may be used to resolve a 2- or 3-dimentional flow velocity vector. As hydroacoustic transducers became available researchers began to investigate the amplitude of backscattered sound at the transducer as a surrogate for sediment concentration. In an early investigation in fluvial environments, Braithwaite (1974) measured SSC and backscatter amplitude from a 1MHz transducer in seven rivers in England and found good qualitative correlation between backscatter amplitude and sediment concentration in fluvial environments. Investigations in marine environments using single-frequency acoustic backscatter include those of Young et al. (1982), Hay (1983), and Hess and Bedford (1985). Flagg and Smith (1989) showed good correlations between acoustic backscatter amplitude and zooplankton abundance with high temporal and spatial resolution.

METHODS USING ACOUSTIC SURROGATES

Semi-empirical method A semi-empirical backscattering theory and acoustic surrogate methodology was progressively developed by several researchers (Sheng and Hay, 1988; Thorne et al., 1991; Hay and Sheng, 1992; Downing et al, 1995; Crawford and Hay, 1993; Thorne and Hardcastle, 1997). This methodology has been tested across a wide range of frequencies and sediment sizes in laboratory and marine environments by these and other authors (Hamilton et al., 1998; Holdaway et al, 1999; Thorne and Hanes, 2002). Fluvial environments have rarely been evaluated. This method estimates the average (root mean square) backscatter amplitude (P_{rms} as pressure) from an ensemble of measurements for a specific ensonified volume, expresses as:

$$P_{rms} = \frac{K_s K_t}{r\psi}\sqrt{SSC}\; e^{-2r(\alpha_w+\alpha_s)} \qquad (4)$$

where

$$K_s = \frac{<f>}{\sqrt{\rho <a_s>}}, \quad K_t = \frac{0.96 P_o r_o}{k a_t}\left\{\frac{3\tau c}{16}\right\}^{0.5}, \quad \psi(r) = 1 + \frac{1}{(1.35 r/r_n) + (2.5 r/r_n)^{3.2}}$$

where, r is the range from the transducer to the ensonified volume, SSC is the mass concentration of suspended sediment, α_w, is the water absorption coefficient, K_s and K_t account for sediment scattering and instrument effects, and $\psi(r)$ accounts for nonuniform energy spreading in the transducer near field, r_n, which is also known as the Rayleigh distance. Other parameters are as defined earlier in this paper. Equation 4 is dimensionally inconsistent.

Water absorption is a function of water temperature, salinity, and pressure and can be obtained by equations or tables (Ainslie and McColm, 1998; Fisher and Simmons, 1977). For most freshwater fluvial environments (at depths less than 100 meters), only temperature will significantly affect α_w .

The parameter K_s accounts for variations due to the size, density, and scattering properties of the sediment, in which $<f>$ is the mean form function for the suspended sediment taken over the range of sediment sizes, ρ is the sediment density, and $<a_s>$ is the mean sediment radius. The variation in form function with particle size and frequency is explored by Thorne and Hardcastle (1997) and Thorne and Hanes (2002). The parameter K_t accounts for variations due to instrument electronic properties and transducer properties in which P_o is the backscatter amplitude at reference distance r_o , usually 1 meter, a_t is the transducer radius, τc is the pulse length equal to the product of pulse duration, τ, and the speed of sound, c.

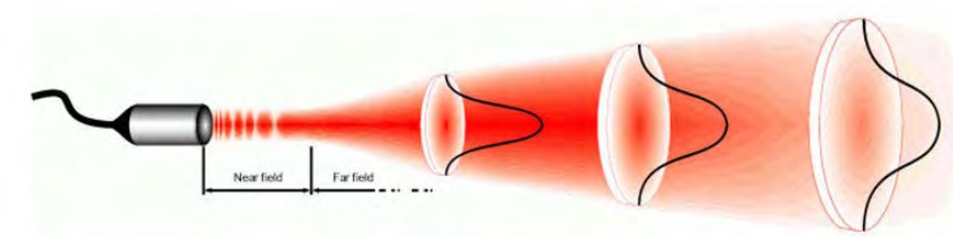

Figure 5 - Decreasing amplitude of acoustic energy by spherical spreading

Backscatter amplitude from reflections in the transducer far field varies with the inverse range (*1/r*) to the measured volume due to spherical spreading of the acoustic energy from the sound source, as illustrated in figure 5. For measurements made near the transducer surface, in the near field, the energy spreading is nonlinear. The parameter $\psi(r)$ accounts for the departure of the acoustic signal from spherical spreading in the near field, $r_n = \pi a_t^2 / \lambda$. In marine studies, transducers often are down-looking from a frame resting on the ocean floor, so that near field corrections often are needed. In fluvial studies, the measurement volume may be beyond the near field, but near field correction will be included here for completeness.

The P_{rms} of equation 4 results from averaging P^2 over several realizations and integrating over the ensonified volume. The conversion from the mean backscattered pressure of individual particles to mass concentration contains an implicit sediment density and equivalent spherical size. Particles within the measurement volume are assumed to be randomly and uniformly distributed, which is likely for measurements from profiling, multi-cell ADCPs, in which the return signal is evaluated (digitally sliced) into smaller, user-specified cell lengths (a pulse time slice). The effects of irregular sediment shape and density are discussed later. Rearranging, equation 4 may expressed as:

$$SSC = \left[\frac{P_{rms}\, r\, \psi}{K_s K_t} \right]^2 e^{4r(\alpha_w + \alpha_s)} \qquad (5)$$

The limitations of this methodology are obvious in that information for the unknown sediment size and SSC are needed to evaluate the K_s and α_s parameters on the right hand side of the equation. These will be discussed further in the limitations section. Investigators using equation 5 have evaluated K_T, K_s and α_s using laboratory measurements and assumptions, with α_s often assumed to be negligible. Potential attenuation due to turbulence was not considered to be significant by any of the reviewed studies.

Urick's Method A different expression relating acoustic surrogates to sediment concentration begins with Urick's (1975) sonar equation and has been used by several authors (Thevenot and Kraus, 1993; Reichel and Nachtnebel, 1994; Gartner, 2004; Wall et al, 2006, Topping et al, 2007). The sonar equation is written in logarithmic units of decibels as:

$$RL = SL - 2TL + TS \qquad (6)$$

where

$$2TL = 20\log_{10}(\psi r) + 2r(\alpha_s + \alpha_w) \qquad (7)$$

In this method *RL* is the reverberation level (intensity) of the received signal and is equal to $10\log_{10}(P_{rms}^2)$, SL is the source level of the emitted signal, *2TL* is the two-way transmission loss equal to the sum of the spherical spreading and attenuation, and *TS* is the intensity of the signal echoed by the particles in the ensonified volume, equal to $10\log_{10}(SSC)$. Equation 6 can be derived from equation 4, except for parameters K_t and K_s, which are handled empirically by most authors using this method, and source level (*SL*) which is generally not evaluated in this method (Thevenot and Krause, 1993; Gartner, 2004). The relative backscatter is computed as $RB = RL+2TL$, which is equivalent to the total scattering by suspended particles. Then, $\log_{10}(SSC)$ is a function of *RB* and:

$$SSC = 10^{(A+B*RB)} \quad (8)$$

The coefficients *A* and *B* are evaluated using regression for paired physical *SSC* and surrogate acoustic measurements. Source level is generally not evaluated in this method (Thevenot and Krause, 1993; Gartner, 2004), and sediment acoustic attenuation is sometimes assumed to be negligible (Gartner and Cheng, 2001; Wall et al., 2006).

Gartner (2004) described the methodology and accounted for water absorption, spreading loss, near field distortion, receiver signal sensitivity, and sediment absorption using Urick's (1948) equation. Gartner used downward looking 1.2 and 2.4 MHz, 4 transducer, broadband acoustic doppler current profilers (ADCPs), mounted about 2 meters above the bed at two locations in San Francisco Bay and calibrated the systems using optical backscatter (OBS) turbidity readings adjacent to the ADCPs. Estimates of SSC of clay to fine sand sizes from acoustic surrogates agreed to within about 8 to 10 percent of those estimated by OBS.

Wall et al. (2006) used an up-looking, bottom mounted, broadband, 4 transducer, 0.614 MHz ADCP on the Hudson River at the USGS stream gage 01372058. They collected concurrent SSC samples from the ensonified volume to calibrate the sonar equation. They also measured depth and width integrated SSC for the stream cross section and developed the relation between sediment flux in the acoustic sampling area and in the river cross section. Their work resulted in the computation of daily sediment flux for this tidally affected reach of the Hudson River which is shown in near real time on the USGS data National Water Information System website (*http://waterdata.usgsgov/nwis).*

Multi-Cell Methods Topping et al. (2007) observed that acoustic attenuation could be measured from multi-cell acoustic return data as the slope of the adjusted signal amplitude loss. Figure 6 shows the acoustic backscatter in decibels (dB) measured by a 3.0 MHz unit with 10 cells of 20cm radial distance each measured between 0.2 and 2.2 meters from the transducer face. The average SSC in the channel cross section was about 694 mg/L at the time of this acoustic measurement. The measured values are assigned to the center location of each cell and the near field boundary for this instrument is 0.77 m. The RL line is the measured backscatter intensity and its slope is the combined two-way signal strength loss due to spherical spreading plus fluid and sediment acoustic attenuation. The ($RL+20\log_{10}(\psi r)$) line is the measured backscatter intensity corrected for spherical spreading and the ($RL+20\log_{10}(r) + r\,\alpha_w$) line is further corrected for fluid attenuation. Solving for the slope of this line provides the two-way acoustic attenuation, $2\alpha_s$. Topping et al. (2004, 2006, 2007) first used this method to solve for α_s. The sediment acoustic attenuation is then used to compute the relative backscatter (RB=RL+2TL) for each cell as shown. The RB for a given cell varies with scattering properties of the ensonified volume, having been corrected for all other factors. This analysis is performed for each time step to obtain a time series of the acoustic attenuation by sediments and normalized acoustic backscatter.

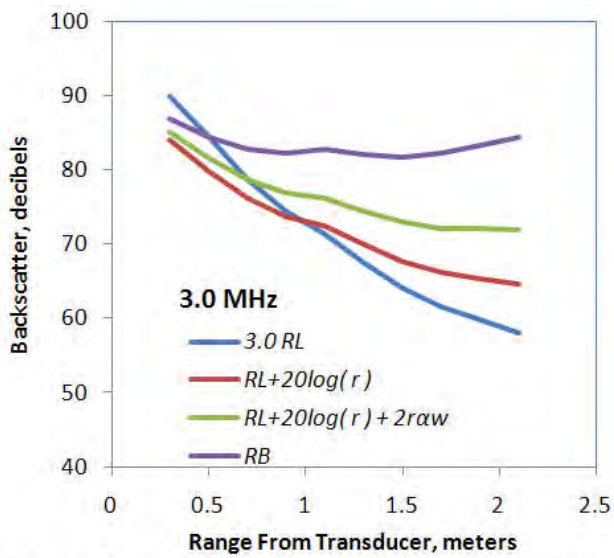

Figure 6 - Backscatter amplitude profiles along axial range for 3.0 MHz transducer

This multi-cell method also has the powerful advantage of normalizing for the effects of sediment scattering properties, K_s, and transducer specific properties, K_t. The effects of K_t would be constant from cell-to-cell in the same measurement, as would the effects of K_s, so long as sediment scattering properties are not changing significantly along the acoustic beam. In other approaches these effects have been assumed to be constant over time, but this method can be applied to normalize measurements at each time-step so that changing sediment scattering properties or changes due to power supply variations can be accounted for.

Multi-Frequency Acoustic Methods A significant limitation of single-frequency systems is that the metrics of acoustic attenuation and backscatter amplitude may change due to changes in sediment concentration or sediment size, creating a size-concentration ambiguity. The amplitude of acoustic backscatter from sediment may increase

with increased concentration at a fixed size distribution or with increased sediment size at a fixed concentration; and acoustic attenuation also varies with size as discussed previously. Multi-frequency acoustic systems, however, have been successfully used to estimate both sediment concentration and size characteristics (Crawford and Hay, 1993; Gartner, 2004; Hay and Sheng, 1992; Thorne et al., 1991; Thorne and Hardcastle, 1997; Smith et al, 2006; Topping et al., 2007). Two approaches have been developed that use multi-frequency acoustics to evaluate sediment size, one by Hay and Sheng (1992) and one by Topping et al. (2007).

In the multi-frequency method developed by Hay and Sheng (1992) and further described by others (Crawford and Hay, 1993; Thorne et al., 1991; Thorne and Hardcastle, 1997; and Thorne and Hanes, 2002), sediment size is obtained from the ratio of form function at different frequencies by inversion of equation 4 as:

$$\frac{< f_i >}{< f_j >} = \left[\frac{P_{rmsi} / K_{ti}}{P_{rmsj} / K_{tj}} \right]^2 e^{2r(\alpha_i - \alpha_j)} \qquad (9)$$

in which

$$< f_i > = 1.1 \left\{ 1 - 0.25 e^{-\left(\frac{ka_s - 1.4}{0.5}\right)^2} \right\} \left\{ 1 + 0.37 e^{-\left(\frac{ka_s - 2.8}{2.2}\right)^2} \right\} \left\{ \frac{1.1(ka_s)^2}{1 + 1.1(ka_s)^2} \right\} \qquad (10)$$

where k is the wave number, as before, i and j refer to different frequencies, and $\alpha = (\alpha_w + \alpha_s)$.

Hay and Sheng (1992) developed and applied a multi-frequency acoustic backscatter system to measure vertical profiles of sand concentration and size near the sea bed (<1 meter) using 1, 2.25, and 5MHz systems. The system was calibrated in the laboratory for individual transducer sensitivity; and for the backscatter from non-spherical scatterers. Hay and Sheng also deployed OBS turbidity sensors near the monitoring bins of the acoustic system. Their laboratory measurements indicated that the three frequency system was able to measure mean concentration with about 10 percent accuracy and mean size with 10 to 20 percent accuracy. The method required averaging measurements over about one-half hour to obtain this accuracy because of high measurement variance. Field measurements indicated that concentrations from the multi-frequency acoustic system and the optical backscatter sensors were within 10 percent. The OBS turbidity sensors were calibrated in the laboratory with local bottom sediments. Smith et al. (2006) apply a similar approach using form-factor ratios to estimate particle sizes for natural sands using a multi-frequency transducer measuring suspensions in a turbulent jet in a laboratory. They found maximum errors of 36 percent for particle diameters from 300 to 950 μm and 160 percent for particle diameters of 150 to 300 μm.

Three frequencies have been used in most multi-frequency sediment surrogate studies. In some applications with little silt and clay, sediment acoustic attenuation is assumed to be negligible and $<a_s>$ can be extracted from the form function ratio at different frequencies (Thorne and Hanes, 2002). As noted in Thorne and Hardcastle (1997) the form function to sediment size relationship for a given frequency is not always monotonic so that multiple solutions are possible; but this can normally be resolved if at least three frequencies are used. Also, the ratio of the form function to sediment size only varies over a limited range of the product of the wave number and sediment size. If $k<a_s>$ is larger than about 2 or less than about 0.2, then there is no size information in $<f_i>/<f_j>$.

Topping et al. (2004, 2006, 2007) have used laser and acoustic metrics as surrogates of suspended sediment for the Colorado River in the Grand Canyon, Arizona, USA. In this river, sediment load is typically controlled by the supply of sediment (supply limited) rather than by the capacity of the flow (capacity limited). Thus, discharge is not a good surrogate of sediment concentration and flux. The suspended sediment size distribution in the study reach is typically bimodal and is highly variable depending on rainfall patterns in the watershed. The calibration data set has silt and clay concentrations from 10mg/L to 20,000 mg/L with median size of 14 μm, and sand concentrations from 10mg/L to 3,000 mg/L, with maximum size of about 150 μm.

Topping et al. (2007) observe the transition from viscous to scattering losses in sediment acoustic attenuation as noted previously for Urick's equation (figure 2) and from this describe two acoustic size classes of sediment; a finer acoustic size class in which viscous attenuation is dominant and a coarser acoustic size class in which scattering attenuation is dominant and backscatter is more significant. The upper limit of the finer acoustic size class is frequency dependent and is defined as 62.5 μm for 2 MHz; 105 μm for 1 MHz, and 177 μm for 0.6 MHz. The range of coarser acoustic size class assigned to each frequency is 62.5-105 μm for 2 MHz, 105-177 μm for 1 MHz, and greater than 177 μm for 0.6 MHz.

In the method developed by Topping et al. (2007) the sediment acoustic attenuation coefficient is determined from multi-cell measurements as described in the previous section and a regression equation is developed between measured silt-clay concentration (less than 63 μm) and α_s for the 2 MHz frequency to obtain a predictive surrogate relation for the concentration of fines. Next, the measured backscatter is normalized for spherical spreading, water attenuation, sediment acoustic attenuation, and a factor for the influence of the fine sediments on increased backscatter for each frequency. Measured sand concentration within the frequency-specific coarse size class is then regressed against this normalized backscatter for each frequency. The total suspended sand concentration is obtained as the sum of the computed concentrations of sand in each grain-size range. The median sand grain size is computed by logarithmic interpolation between the acoustically computed concentrations in each grain-size range. Applying this method, Topping et al. (2007) report computed concentrations within 5% of the values computed using conventional data; and median sand grain size typically within 10% of the values obtained by conventional measurement.

Limitations and Assumptions of Acoustic Surrogates As discussed previously, acoustic metrics from single-frequency systems may change due to changes in sediment concentration or sediment size, creating a size-concentration ambiguity. This limitation may be overcome using multi-frequency acoustic systems, although these systems will increase complexity and cost. Acoustic metrics are sensitive to the ratio of sediment size to wave number and a somewhat narrow frequency is optimal for evaluation of particle size distribution using multi-frequency acoustics (Gray and Gartner, 2009). The sensitivity of acoustic surrogates of suspended sediment is limited for low concentrations and generally may not be applicable for concentrations less than about 10 mg/l for frequencies in the 0.5 to 5MHz frequency range (Gray and Gartner, 2009). All methods that use measurements of a subsection of the channel cross section involve assumptions that the relation of concentrations in the subsection and in the full cross section is stable for periods between recalibration. This limitation is more restrictive for surrogates based on small point volume measurements than for acoustic surrogates which typically are based on a much larger volume than point measurements.

The irregular shape of natural sediments can significantly affect acoustic backscatter and attenuation. Two particle shape characteristics of natural sediments affect acoustic surrogates. The backscatter cross section, or the effective particle area incident to the acoustic wave, affects the backscattered energy; and the total scattering cross section, which affects the energy scattered in all directions (Hay and Sheng, 1992). Expressions for the effects of irregular shaped particles on acoustic scattering were developed by Sheng and Hay (1988).

Because the semi-empirical method requires estimation of K_S and K_T, additional assumptions are required that are not required where these affects are normalized for empirically using the multi-cell approach. Knowledge or assumptions of SSC, particle size, and particle scattering characteristics are required to compute K_s. Throne and Hanes (2002) review methods such as estimating sediment size from bed-material samples, assuming α_s is negligible, and solving equation 4 using an iterative approach. In fluvial environments, scattering characteristics likely would be more variable in than in marine environments, increasing uncertainty in K_s estimates.

Full electronic and acoustic evaluation of K_t requires measurements of the transmit signal level, receiver amplification, time variable electronic gain, analog to digital conversion, and the transducer beam pattern. These characteristics can vary with power supply and environmental conditions, and characteristics for each transducer are unique, even for the same multi-transducer instrument. Experimental determination of these characteristics is very difficult and requires specialized laboratory instrumentation (Holdaway et al, 1999; Thorne and Hanes, 2002). K_s and K_t have often combined into a single calibration coefficient because of their complexity and because they may have a limited variance in specific marine sediment conditions for a single, specialized instrument set up.

FIELD INVESTIGATION USING ACOUSTIC SURROGATES

A field investigation is began in 2009 to evaluate methods to determine fluvial suspended sediment characteristics by high-resolution, surrogate metrics of multi-frequency acoustic, turbidity, and laser-diffraction properties. Physical samples of suspended sediment are being collected concurrently with surrogate metrics from instruments including 1.2, 1.5, and 3.0 MHz frequency, 2 transducer ADCPs, a nephelometric turbidity sensor, and a laser-diffraction particle size analyzer.

The investigation is being conducted at the Yellow River at Gees Mill Road, near Milstead, Georgia (USGS stream gage 02207335), which has a 260 square mile watershed originating in northeast metropolitan Atlanta. The watershed has a developing urban land use with about 16 percent impervious surfaces in 2000, based on the National Land Cover Dataset (MLRC, 2001). At this location stage, discharge, precipitation, and nephelometric turbidity are continuously monitored. Mean and maximum suspended sediment concentrations observed at this site are 144 and 982 mg/L, respectively, based on 65 samples collected from 2002 to 2008. Suspended sediment is predominantly silt-clay and fine sand. The first fully sampled storm occurred in August 2009 during which concurrent, continuous surrogates were measured and more than 75 physical sediment samples were collected. Results will be reported in future papers as additional data collection and analyses are completed.

Physical sediment samples will be collected using a fixed-point pumping sediment sampler and using depth and width integrated sampling methods described by Edwards and Glysson (1999). Fixed point samples will be obtained every one to two hours during sampled events and used to estimate channel cross section SSC based on the relation of fixed point sample SSC to concurrent cross-section average SSC.

Figure 7- Acoustic doppler current profilers mounted on downstream bridge pier at west edge of main channel

Three horizontal-looking ADCPs have been deployed for this investigation. Two are manufactured by Sontek, Incorporated and are a 1.5 MHz Sontek Argonaut SL and a 3.0 MHz Sontek Argonaut SW. The third unit is manufactured by Teledyne RD Instruments (RDI) and is a 1.2 MHz RDI Channel Master H-ADCP. They have been mounted on the downstream side of a bridge pier located on the west bank of the Yellow River at Gees Mill Road (figure 7). The meters record the average of measurements over 120 seconds every 15 minutes. The measurement initiation time for each meter was offset by 5 minutes to eliminate any potential problems with acoustic interference between the meters.

Methods to estimate sediment characteristics from the acoustic metrics of attenuation and backscatter have been developed and tested over several decades. The two principal methods of estimating sediment characteristics from acoustic surrogates can be mathematically equated. The results of the literature search suggest that these surrogate methods could provide improved information of higher resolution and potentially lower cost, to inform solutions to increasing sedimentation issues.

REFERENCES

Ainslie, M. A., and McColm, J. G. (1998), A simplified formula for viscous and chemical absorption in sea water. J. Acoustical Society of America, 103 (3), 1671-1672

Braithwaite, H. (1974), Some measurements of acoustic conditions in rivers. J. of Sound and Vibration, 37, 557-560

Conner, C. S. and A. M. De Visser (1992), A laboratory investigation of particle size effects on optical backscatterance sensor. Mar. Geol., 108, 151-159

Crawford, A. M. and Hay, A. E. (1993). Determining suspended sand size and concentration from multi-frequency acoustic backscatter. Journal of the Acoustical Society of America, 94, 3312-3324

Downing, J. P., Sternberg, R. W. and Lister, C. R. B. (1981), New instrumentation for the investigation of sediment suspension processes in the shallow marine environment. Mar. Geol., 42, 19–34.

Downing, A., Thorne, P. D. and Vincent, C. E. (1995), Backscattering from a suspension in the near field of a piston transducer. J. Acoust. Soc. Am. 97, 1614–1620.

Downing, J. P. (1996), Suspended sediment and turbidity measurements in streams: What they do and do not mean. Automatic Water Quality Monitoring Workshop, Richmond, B.C., 12–13 February.

Edwards, T. E., and Glysson, G. D. (1999), Field methods for collection of fluvial sediment. U.S.G.S. Techniques of Water-Resources Investigations Book 3, Chp C2, 89 p.

Fisher, F. H., and Simmons, V. P. (1977), Sound absorption in sea water. J. Acoustical Soc. Am., 62 (3), 558-564

Flagg, C. N. and Smith, S. L. (1989), On the use of the acoustic Doppler current profiler to measure zooplankton abundance. Deep-Sea Res., 36, 455–474

Flammer, G. H. (1962), Ultrasonic measurement of suspended sediment. U.S.G.S. Bul. 1141–A, 48 pp

Gartner, J. W. and Cheng, R. T. (2001), Promises and Pitfalls of estimating TSS from Backscatter. Proceedings of the 7th Federal Interagency Sedimentation Conference, Vol. III, Reno, Nevada, 25-29

Gartner, J. W. (2004), Estimating suspended solids concentrations from backscatter intensity measured by acoustic Doppler current profiler in San Francisco Bay, California. Marine Geology, 211, 169–187

Gray, J. R., and Gartner, J. W. (2009) Technological advances in suspended-sediment surrogate monitoring. Water Resources Research., 45, W00D29

Hamilton, L. J., Shi, Z. and Zhang, S. Y. (1998). Acoustic backscatter measurements of estuarine suspended cohesive sediment concentration profiles. J. of Coastal Res., 14, 1213-1224.

Hay, A. E. (1983), On the Remote Acoustic Detection of Suspended Sediment at Long Wavelengths. J. Geophys. Res., 88(C12), 7525–7542

Hay, A. E. and Sheng, J. (1992), Vertical profiles of suspended sand concentration and size from multi-frequency acoustic backscatter. J. of Geo. Res., 97, 15661-15677.

Hess, F. R., and Bedford K. W. (1985), Acoustic Backscatter System (ABSS): The instrument and some preliminary results. Marine Geology, 66, 357-379

Holdaway, G. P., Thorne, P. D., Flatt, D., Jones, S. E. and Prandle, D. (1999), Comparison between ADCP and transmissometer measurements of suspended sediment concentration. Con. Shelf Res., 19, 421–441

Horowitz, A. J. (1991), A primer on sediment-trace element chemistry: Second ed., Chelsea, Mich., Lewis Publishers, 136 p.

Horowitz, A. J., Elrick, K. A., Smith, J. J. (2008), Monitoring urban impacts on suspended sediment, trace element, and nutrient fluxes within the City of Atlanta, Georgia, USA: program design, methodological considerations, and initial results. Hydrological Processes, 22, 1473–1496

Jean P. G., Minella, G., Merten, H., Reichert, J. M., Clarke, R. T. (2008), Estimating suspended sediment concentrations from turbidity measurements and the calibration problem. Hydrological Processes, 22

Lamb, H. (1916), Hydrodynamics, 4th edition, Cambridge University Press, 708pp

Landers, M. N. (2003), Summary of blind sediment reference sample measurement session. Proceedings of the Federal Interagency Workshop on Turbidity and Other Sediment Surrogates, Reno, Nevada, 30 April-2 May, U.S.G.S. Circular 1250, 29-30.

Lewis, J. (1996), Turbidity controlled suspended sediment sampling for runoff event load estimation. Water Resources Research, 32, 2299–2310.

Lynch, J.F., Irish, J.D., Sherwood, C.R., Agrowal, Y.C. (1994), Determining suspended sediment particle size information from acoustical and optical backscatter measurements. Continental Shelf Research 14 (10/11), 1139-1165.

Multi-Resolution Land Characteristics (MRLC) Consortium (2001), National Land Cover Database 2001. <http://www.mrlc.gov/mrlc2k_nlcd.asp>

Rasmussen, P. P., Gray, J. R., Glysson, D. G., and Ziegler, A. C. (2009), Guidelines and Procedures for Computing Time-Series Suspended-Sediment Concentrations and Loads from In-Stream Turbidity-Sensor and Streamflow Data. U.S.G.S. Techniques and Methods Report Book 3, Chapter C4, 66p

Rayleigh, Lord (J. W. Strutt) (1896), Theory of Sound, Macmillan and Co. Ltd, New York, 2, 2nd ed., 504 pp

Reichel, G., and Nachtnebel, H. P. (1994), Suspended sediment monitoring in a fluvial environment: Advantages and limitations applying an acoustic Doppler current profiler. Water Resources, 28, 751-761

Sewell, C. J. T. (1910), The extinction of sound in a viscous atmosphere by small obstacles of cylindrical and spherical form: Philosophical Transactions of the Royal Soc. of London, Series A, 210, 239-270

Sheng, J. and Hay, A. E. (1988), An examination of the spherical scatter approximation in aqueous suspensions of sand. J. Acoust. Soc. Am., 83(2), 598-610.

Simpson, M. R. (2001) Discharge measurements using a broad-band acoustic doppler current profiler, U.S.G.S. Open File Report 01-1, 123 pp

Smith, C. K., Wren, D., and Chambers, J. (2006), Estimation of particle sizes for a range of narrow size distributions of natural sands suspended in water using multi-frequency acoustic backscatter. Proceedings of the 8th Federal Inter-Agency Sedimentation Conference, Reno, NV, April 2–6, 2006, 531–538

Sutherland, T. F., Lane, P. M., Amos, C. L. and Downing, J. (2000), The calibration of optical backscatter sensors for suspended sediment of varying darkness levels. Mar. Geol. 162, 587-597

Thevenot, M. M., and Kraus, N. C. (1993), Comparison of acoustical and optical measurements of suspended material in the Chesapeake Estuary. J. Mar. Env. Eng., 1, 65-79.

Thorne, P. D., Vincent, C. E., Harcastle, P. J., Rehman, S. and Pearson, N. (1991), Measuring suspended sediment concentrations using acoustic backscatter devices. Mar. Geol., 98, 7-16.

Thorne, P. D. and Hardcastle, P. J. (1997), Acoustic measurements of suspended sediments in turbulent currents and comparison with in-situ samples. Journal of the Acoustical Society of America, 101, 2603-2614

Thorne, P.D. and Hanes, D.M. (2002), A review of acoustic measurement of small-scale sediment processes, Continental Shelf Research, 22, 603-632

Topping, D. J., Melis, T. S., Rubin, D. M. and Wright, S. A. (2004), High-resolution monitoring of suspended-sediment concentration and grain size in the Colorado River in Grand Canyon using a laser acoustic system, in Proceedings of the 9th International Symposium on River Sedimentation, Yichang, China, 18-21 October, Tsinghua University Press, 2507-2514.

Topping, D. J., Wright, S. A., Melis, T. S., and Rubin, D. M. (2006), High-resolution monitoring of suspended-sediment concentration and grain size in the Colorado River using laser-diffraction instruments and a three-frequency acoustic system. Proceedings of the 8th Federal Inter-Agency Sedimentation Conference, Reno, NV, April 2–6, 2006, 555–559

Topping, D. J., Wright, S. A., Melis, T. S. and Rubin, D. M. (2007), High-resolution measurement of suspended-sediment concentrations and grain size in the Colorado River in Grand Canyon using a multi-frequency acoustic system, in Proceedings of the 10th International Symposium on River Sedimentation, Moscow, Russia, 1-4 August, 330-339

Uhrich, M. A., and H. M. Bragg (2003), Monitoring instream turbidity to estimate continuous suspended-sediment loads and yields and clay-water volumes in the Upper North Santiam River Basin, Oregon, 1998–2000, U.S. Geol. Surv. Water-Resources Investigations Report 03-4098, 44 pp.

Urick, R.J. (1948), The absorption of sound in suspensions of irregular particles, Acoustical Soc. of America, 20, 283-289

Urick, R. J. (1975), Principles of underwater sound, 2nd ed., McGraw Hill, N. Y., 384 pp.

U. S. Environmental Protection Agency (2008), Handbook for Developing Watershed Plans to Restore and Protect Our Waters, Office of Water, Nonpoint Source Control Branch, EPA 841-B-08-002, 400 pgs

Wall, G. R., Nystrom, E. A., and Litten, S. (2006), Use of an ADCP to Compute Suspended-Sediment Discharge in the Tidal Hudson River, New York, USGS SIR 2006-5055

Walling, D. E. (1977), Assessing the Accuracy of Suspended Sediment Rating Curves for a Small Basin, Water Resour. Res., 13(3), 531–538.

Wood P.J., and Armitage, P.D. (1997) Biological effects of fine sediment in the lotic environment. Environmental Management 21: 203-217

Wright, S.A., and Topping, D.J. (2010), Evaluation of hydroacoustics for monitoring suspended-sediment transport in rivers, http://*hydroacoustics.usgs.gov/training/webinars/SAW-Acoustics-Sediment.ppt, December 2009*

Young, R. A., Merrill, J. T., Clarke, T. L. and Proni, J. R. (1982), Acoustic Profiling of Suspended Sediments in the Marine Bottom Boundary Layer, Geophys. Res. Lett., 9(3), 175–178